

DETERMINATION OF FLOW VELOCITY, TURBULENCE INTENSITY AND LENGTH AND TIME SCALES FROM GAS DISCHARGE PARAMETERS

R. Maly and H. Meinel

Universität Stuttgart, Institut für Physikalische Elektronik,
D 7000 Stuttgart-1, Böblingerstrasse 70.

ABSTRACT

It will be shown by theoretical and experimental investigations that glow and arc discharges may be used to measure all essential flow field properties. Setup and data extraction are very simple. This method may be used also in nontransparent chemically reacting environments (e.g. fired engines, furnaces, plasma reactors) where Hot Wire Anemometry (HWA) and Laser Doppler Anemometry (LDA) are often not applicable. Its capabilities are demonstrated by measurements on a free jet and on 4 stroke engines both fired and unfired.

1. THEORY

A thorough treatment will be found elsewhere /1/, from which the main features are compiled below.

During the breakdown of a conventional spark discharge a channel along the shortest path across the electrode gap establishes within some nanoseconds /2,3/. If an external flow field is present this channel will change its length inertiafree according to the local velocity field. Its ends are, however, still fixed to the electrodes. The increase in channel length requires an increase in power input to the discharge. This gives rise to an increase in the sustaining voltage when a constant current source is used. As the field strength E of the positive column of the glow or arc discharge is constant for a constant current one obtains according to the definitions in Fig. 1a

$$V(t) = V_c + E \cdot l_0 + E \int_0^t dl \quad (1)$$

with V_c = cathode fall and

$$dl = 2\sqrt{(\bar{U} + u_x)^2 + u_y^2 + u_z^2} dt \quad (2)$$

where \bar{U} is the mean flow velocity and u_x, u_y, u_z are the components of the fluctuating part of the general flow velocity $U(r,t)$. After Hinze /4/, $u_j' = (\overline{u_j^2})^{1/2}$ is defined as turbulence intensity and u_j' / \bar{U} , $j = x, y, z$, as turbulence level.

Thus without any further treatment the rate of the velocity increase $\dot{V}(t)$ is directly a function of the flow velocity of the

type being used in HWA:

$$\dot{V}(t) = 2E \sqrt{(\bar{U} + u_x)^2 + u_y^2 + u_z^2} \quad (3)$$

If long electrodes parallel to \bar{U} (see Fig. 1b) are used instead of pin pointed electrodes the resulting sensitivity to the mean velocity \bar{U} is zero and one obtains:

$$\dot{V}(t) = 2E \sqrt{u_x^2 + u_y^2 + u_z^2} \quad (4)$$

For $u_x^2 + u_y^2 + u_z^2 < U^2$, which is true for almost all flow fields, the root in (3) may be expanded into a power series as it is done in HWA. Retaining only the most significant terms one finds:

$$\dot{V}(t) = 2E (\bar{U} + u_x) \quad (5)$$

As u_x may be written also in form of a Fourier series:

$$u = \sum_{i=1}^{\infty} (a_i \sin i\omega t + b_i \cos i\omega t) \quad (6)$$

we finally obtain from N experiments the ensemble average:

$$\bar{U}(\vec{r}_0, t_0) = \frac{1}{2EN} \sum_{i=1}^N V(t_0) \quad (7)$$

and additionally N individual time functions for the turbulence velocity u_{xi} :

$$u_{xi}(\vec{r}_0, t) = \frac{1}{2E} \dot{V}_i(t) - \bar{U}(\vec{r}_0, t_0) \quad (8)$$

Thus we are able to extract the spectral distributions of ω_i (angular velocities of the eddies), u_i (amplitudes of the turbulent velocity) and $r_i = (a_i^2 + b_i^2)^{1/2}$ (radii of the eddies) from a Fourier analysis of u_{xi} . In addition, all the correlation techniques used in HWA are also applicable and provide a complete description of a general flow field.

The field strength E for constant current which is required for the evaluation of numerical values may be provided either by calibration or by the method itself. If changes in pressure, temperature and species occur during the measuring interval, E_i may be determined from:

$$V_i(t_0) = V_c + E_i \cdot l_0 \quad (9)$$

if a 2 electrode system is used and V_c can be assumed constant, or from

$$V_i(t_1) - V_i(t_0) = E_i(l_1 - l_0) \quad (10)$$

if one prefers a 3 electrode system where V_c is allowed to change too /1/.

Thus every individual curve $\dot{V}(t)$ may be evaluated with its appropriate E_i . This is an especially valuable feature of this method

as accurate measurements under virtually all nonsteady environmental conditions are possible.

2. EXPERIMENTAL SETUP

In Fig. 2, the most simple setup required for measuring flow parameters is presented. As a constant current source, a conventional high impedance Transistorized Coil Ignition (TCI) as used in automobiles is satisfactory in spite of its linearly decreasing current characteristic, if all measurements are made at identical current values and during an appropriately short time interval (e.g. 50 μ s). However, combining a TCI with a regulated high voltage constant current source is easily possible [1], so that there are no real limitations to the tolerable time interval for taking measurements.

Pin pointed electrodes and long parallel electrodes made from .3 mm Pt wire were used for measuring mean velocity and turbulence velocities, respectively. The spark is initiated at the desired instant of time. The discharge voltage is then measured by a high voltage probe and preferably a fast digital data acquisition and processing system. However, an oscilloscope and an instant camera will do for a quick overview. The 5 k Ω resistors suppress possible radio interference and further shielding may be required if the spark is not operated in a closed metallic housing.

Usually 15 voltage time functions $V(t)$ were recorded at every measured point. Due to fast initial transients not directly related to the flow field, evaluation started at 50 μ s after spark onset. As test objects, a free air jet issued from a long round tube ($D = 4$ mm, 500 mm long, $\bar{U}_0 = 35$ m/s) in quiescent air at ambient pressure and temperature was used. In Fig. 3, an overview of the jet structure is given along with the long parallel electrode system used for turbulence measurements. The jet was visualized by using He instead of air and taking a shadowgraph. Also given is an impression of the curling effect of eddies on the discharge channel. In Fig. 4, typical traces of $V(t)$ for the two types of electrodes are shown.

3. RESULTS

The results of flow measurements on the free air jet are presented in Fig. 5, 6 and 7. Available data from the literature is included for comparison. As expected from the identity of the used functional relation in HWA and the presented method, one finds a good agreement between all the measured and referenced data even for small values of x/D where wall effects from the tube may be present. The least squares fit of measured data between $x/D = 10$ to 45 indicates a hyperbolic decay of the centerline velocity in accordance with theoretical expectations; however, with a slightly greater slope. This faster decay is primarily due to the limited number of measured data for larger x/D values as the relative scatter of experimental data tends to increase with the distance from the orifice. The underlying reason for this is the increase in eddy size with x/D so that the ensemble averaging should be extended over an increasingly larger number of events in order to assure statistically representative values. This is supported by the almost periodic distribution of data points along the least squares fit.

As has been pointed out by Wagnanski and Fiedler /6/ the rate of growth of the jet is sensitive to the conditions of self preservation, which are felt to differ somewhat from the conditions in the referenced data due to the difference in orifice diameter (4 mm versus 25.4 mm). This is supported by measurements of Plessis et al., who found a faster decay of the center line velocity for small orifices /10/. The shape of the normalized velocity profiles on the other hand is not affected so here an excellent agreement between measured and referenced data is found.

As correlation measurements have not been performed we assumed isotropic turbulence and determined values lying well within Wagnanski and Fiedlers data for u_x and u_y , u_z , respectively. The scatter indicates here also the need for a larger ensemble for evaluation. However, a simple increase in the number of measurements per second is not sufficient as the integral time for measuring flow parameters has to be extended also over a time interval long enough to assure statistical relevance.

The length scales were determined at $x/D = 1.1$ and 4 to be 0.37 mm and 0.53 mm, respectively. They compare favourably with length scales calculated according to Davies /9/: 0.59 mm and 0.78 mm. From Taylors hypothesis we obtain the time scales: 10 μ s and 18 μ s.

The results of an application of the presented measuring technique to real engines are shown in Fig.8. The strong influences of combustion chamber design, swirl and squish flows on the local flow characteristics are clearly resolved. Furthermore, the results demonstrate the necessity to measure flow data under actual conditions as the burning process itself and the local geometry affect the flow field in an unpredictable way.

We conclude therefore that the presented method is a valuable supplement to the available measuring techniques for general flows.

REFERENCES

- /1/ R. Maly and H. Meinel, to be published.
- /2/ R. Maly and M. Vogel, 17th Symp. (Int.) on Combustion, 821 (1978).
- /3/ H. Albrecht, R. Maly, B. Saggau und E. Wagner, Automobil-Industrie, 4/77, 45 (1977).
- /4/ J.O. Hinze, "Turbulence" (McGraw-Hill, New York, 1958).
- /5/ R. Wille, Z. Flugwiss., 11, 222 (1963).
- /6/ I. Wagnanski and H. Fiedler, J. Fluid Mech., 38, 577 (1969).
- /7/ N. Trentacoste and P. Sforza, AIAA Journal, 5, 885 (1967).
- /8/ A. Jogwich, "Strömungslehre" (Giradet, Essen, 1974).
- /9/ P.O.A.L. Davies, M.J. Fisher and M.J. Barrat, J. Fluid Mech., 15, 337 (1963).
- /10/ M.P. du Plessis, R.L. Wang and R. Kahawita, Transactions of the ASME, 246 (1974).

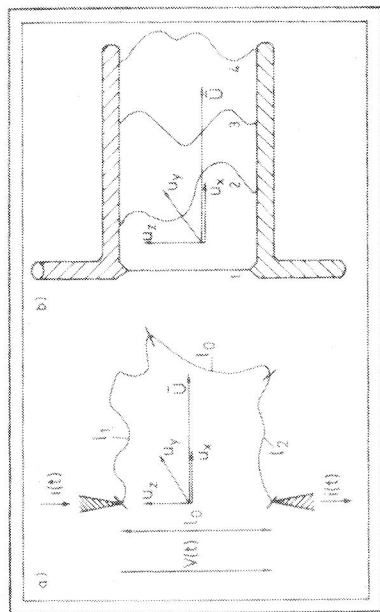


Fig. 1 Effect of a flow field on a glow discharge channel. a: Pin pointed, b: Long parallel electrodes

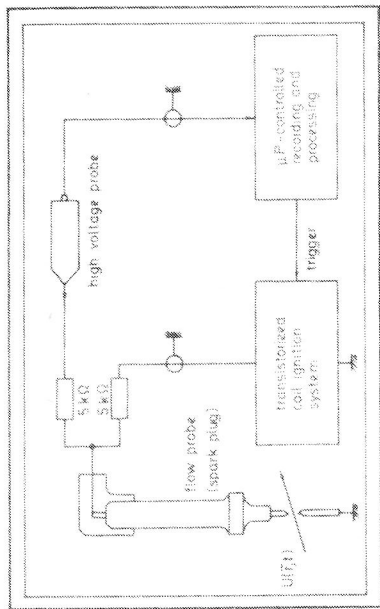


Fig. 2 Schematic measuring setup for flow field investigations by a glow discharge.

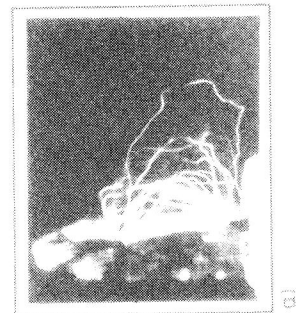


Fig. 3 Prints of a glow discharge channel and the free jet as used in the experiments. a: Multi-exposure print showing turbulence effects, b: Structure of the free jet.

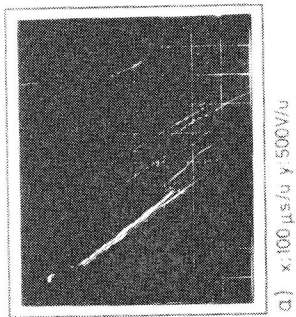
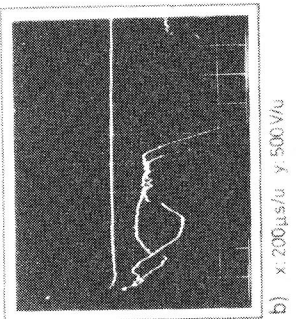


Fig. 4 Voltage time traces of glow discharges in a flow field. a: Laminar flow, pin pointed electrodes, b: Turbulent flow, long parallel electrodes for zero sensitivity to U .



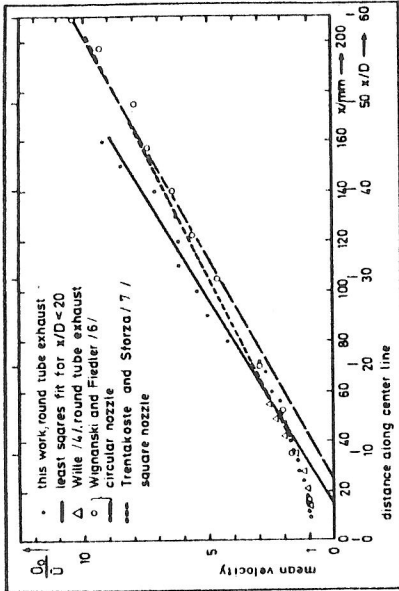


Fig. 5 Decay of mean velocity of a free jet.

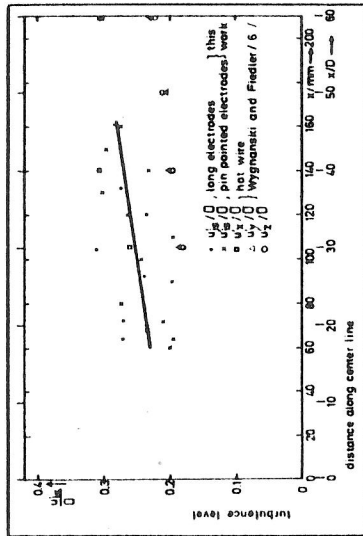


Fig. 7 Turbulence level of a free jet.

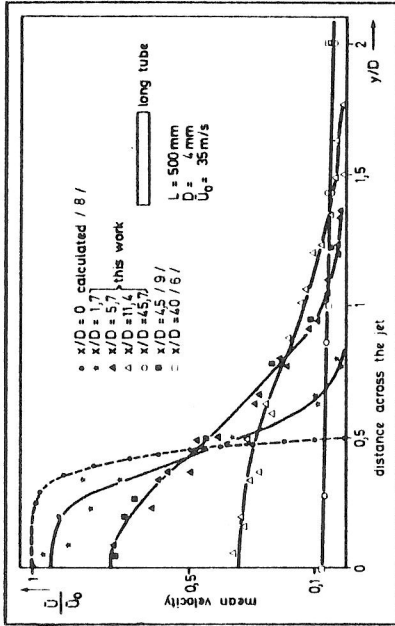


Fig. 6 Radial profiles of mean velocities in the free jet.

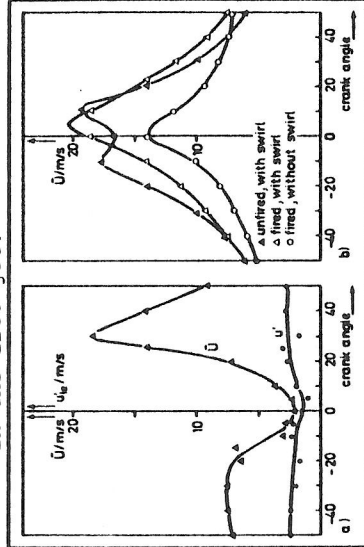


Fig. 8 Mean velocity and turbulence intensity. a: 2kW engine, no swirl, unfired, b: 20 kW engine, effects of swirl and combustion.